

Muons from Neutralino Annihilations in the Sun: Flipped SU(5)

Muhammad Adeel Ajaib,^{*} Ilia Gogoladze^{b,‡} and Qaisar Shafi[§]

*Bartol Research Institute, Department of Physics and Astronomy
University of Delaware, Newark, Delaware 19716*

We consider two classes of supersymmetric flipped SU(5) models with gravity mediated supersymmetry breaking such that the thermal neutralino relic abundance provides the observed dark matter density in the universe. We estimate the muon flux induced by neutrinos that arise from neutralino annihilations in the Sun and discuss prospects for detecting this flux in the IceCube/Deep Core experiment. We also provide comparisons with the corresponding fluxes in the constrained minimal supersymmetric standard model and non-universal Higgs models. Regions in the parameter space that can be explored by the IceCube/DeepCore experiment are identified.

PACS numbers: 95.35.+d, 98.62.Gq, 98.70.Vc, 95.85.Ry

I. INTRODUCTION

It is now widely accepted that approximately 23 % of the Universe's energy density consists of non-baryonic cold dark matter [1]. A large number of experiments consisting of direct, indirect and accelerator searches are currently underway all hoping to discover the underlying, presumably massive (\sim GeV -TeV), weakly interacting dark matter particle (WIMP). The lightest neutralino in supersymmetric models with conserved matter parity is a particularly attractive cold dark matter candidate and has attracted a great deal of attention. The direct detection searches have already yielded important constraints on the spin independent neutralino-nucleon cross sections in the constrained minimal supersymmetric standard model (CMSSM) and some related models (see [2], and references therein).

Indirect WIMP searches rely on the capture and subsequent annihilation, say in the Sun's center, of relic dark matter particles. The neutralinos, in particular, can annihilate into the known SM particles, for example, $\chi\chi \rightarrow \tau^+\tau^-$. The tau particles in turn produce energetic muon neutrinos which interact with the polar ice to produce muons which can be identified by the km³ IceCube/Deep Core detector [3].

Neutralinos in the galactic halo passing through a massive body like the Sun can get captured if they scatter off the nuclei with velocities smaller than the escape velocity. In the core of the Sun, where they eventually accumulate, these neutralinos can annihilate into known SM particles, for e.g., $\chi\chi \rightarrow \tau^+\tau^-$. These particles decay (e.g. $\tau \rightarrow \nu_\tau \bar{\nu}_\mu \mu$) and produce energetic muon neutrinos which can then be detected at IceCube after they interact with the polar ice and produce muons (for e.g. via processes like $\nu_\mu + N \rightarrow \mu^- + X$, N being the nucleon and X some hadronic system). We investigate the possibility of detecting these energetic neutrinos by estimating the flux of muons that they induce. In addition to the well studied CMSSM, we explore other well motivated models, namely, flipped SU(5), non-universal Higgs models (NUHM2), and flipped SU(5) with universal Higgs masses at M_{GUT} . The prospects for detecting this neutrino induced muon flux by the IceCube/DeepCore experiment is discussed.

In this paper we are mainly interested in studying the implications of supersymmetric flipped SU(5) models for indirect dark matter WIMP searches, with the lightest neutralino being the dark matter candidate. Flipped SU(5) has several distinct features which are not easily replicated in other GUTs such as SU(5) and SO(10). For instance, the well-known doublet-triplet splitting problem is easily solved in flipped SU(5) [4]. Primordial inflation with predictions for the cosmological parameters in good agreement with the 7 year WMAP data are readily obtained, which in turn, lead to testable predictions for proton decay [5].

Our paper is organized as follows. In section II, following [6], we briefly describe the two flipped SU(5) models under discussion. Consistent with the underlying gauge group (SU(5) x U(1)), both classes of models work with non-universal gaugino masses. Their difference stems from the non-universal soft scalar Higgs masses employed in one of the models. In section III we review the calculations of the conversion factors relating the muon flux and spin dependent (SD) cross section in the IceCube/Deep Core experiment. Section IV contains a description of the experimental constraints and the scanning procedure employed to generate the benchmark points. Our predictions for the muon flux and SD cross section are presented in section V, and the conclusions are summarized in section VI.

^b On leave of absence from: Andronikashvili Institute of Physics, GAS, Tbilisi, Georgia.

^{*} adeel@udel.edu

[‡] ilia@bartol.udel.edu

[§] shafi@bartol.udel.edu

II. THEORETICAL FRAMEWORK OF THE MODELS

We are interested in estimating the neutrino induced muon fluxes from neutralino annihilations in the Sun, with flipped SU(5) (FSU(5)) boundary conditions imposed on the soft supersymmetry breaking (SSB) parameters at M_{GUT} . More generally, we compare four distinct models, namely CMSSM, NUHM2, FSU(5) and FSU(5) with Universal SSB Higgs mass boundary condition (FSU(5)-UH). We will briefly describe each model below. The CMSSM [7] has the following parameters at the M_{GUT} :

$$m_0, m_{1/2}, A_0, \tan\beta, \text{sign}(\mu). \quad (1)$$

Here m_0 is the soft supersymmetry breaking (SSB) scalar masses, $m_{1/2}$ is the SSB gaugino mass, A_0 is the universal SSB trilinear scalar interaction (with the corresponding Yukawa coupling factored out), $\tan\beta$ is the ratio of the vacuum expectation values (VEVs) of the two MSSM Higgs doublets, and the magnitude of μ , but not its sign, is determined by the radiative electroweak breaking (REWSB) condition.

Whereas, universal scalar masses are motivated to suppress unwanted flavor changing neutral currents, the Higgs mass parameters can be non-universal. The effects of this non-universality on the parameter space has been studied in models called Non-Universal Higgs Models (NUHM) [8]. One of the types of these models called the NUHM2 has two additional parameters compared to the CMSSM

$$m_{H_u}^2, m_{H_d}^2, \quad (2)$$

where $m_{H_u}^2$ and $m_{H_d}^2$ are the SSB the MSSM Higgs mass² term. The supersymmetric flipped SU(5) (FSU(5)) model [9] is based on the maximal subgroup $G \equiv \text{SU}(5) \times \text{U}(1)_X$ of SO(10), and the sixteen chiral superfields per family of SO(10) are arranged under G as: $10_1 = (d^c, Q, \nu^c)$, $\bar{5}_{-3} = (u^c, L)$, $1_5 = e^c$. Here the subscripts refer to the respective charges under $\text{U}(1)_X$, and we follow the usual notation for the Standard Model (SM) particle content. The MSSM electroweak Higgs doublets H_u and H_d belong to $\bar{5}_H$ and 5_H of SU(5), respectively. We will assume for simplicity that the soft mass² terms, induced at M_{GUT} through gravity mediated supersymmetry breaking [10], are equal in magnitude for the scalar squarks and sleptons of the three families. The asymptotic MSSM gaugino masses, on the other hand, can be non-universal. Due to the FSU(5) gauge structure, asymptotic $\text{SU}(3)_c$ and $\text{SU}(2)_W$ gaugino masses can be different from the $\text{U}(1)_Y$ gaugino mass. Assuming SO(10) normalization for $\text{U}(1)_X$, the hypercharge generator in FSU(5) is given by $Y = (-Y_5/2 + \sqrt{24}X)/5$, where Y_5 and X are the generators of SU(5) and $\text{U}(1)_X$ [11]. We then have the following asymptotic relation between the three MSSM gaugino masses:

$$M_1 = \frac{1}{25}M_5 + \frac{24}{25}M', \text{ with } M_5 = M_2 = M_3, \quad (3)$$

where M_5 , M' , M_3 , M_2 and M_1 denote SU(5), $\text{U}(1)_X$, $\text{SU}(3)_c$, $\text{SU}(2)_L$ and $\text{U}(1)_Y$ gaugino masses respectively. The supersymmetric FSU(5) model thus has two independent parameters ($M_2 = M_3$, M') in the gaugino sector. In other words, in FSU(5), by assuming gaugino non-universality, we increase by one the number of fundamental parameters compared to the CMSSM

We will also consider both universal ($m_{H_u}^2 = m_{H_d}^2$) and non-universal ($m_{H_u}^2 \neq m_{H_d}^2$) soft scalar Higgs masses in FSU(5), using the notations for FSU(5)-UH and FSU(5) respectively. This would mean up to three additional parameters compared to the CMSSM. This latter case, with one additional gaugino mass parameter and two soft scalar mass parameters, provides us with a compelling neutralino dark matter candidate for indirect and direct detection [6] in the ongoing and future experiments.

We use the (μ, m_A) parameterization to characterize non-universal soft scalar Higgs masses rather than (H_u, H_d) . The fundamental parameters of our FSU(5) model are

$$m_0, M', M_2, \tan\beta, A_0, \mu, m_A, \quad (4)$$

we will assume that $\mu > 0$. Note that μ and m_A are specified at the weak scale, whereas the other parameters are specified at M_{GUT} . Although not required, we will assume that the gauge coupling unification condition $g_3 = g_1 = g_2$ holds at M_{GUT} in FSU(5). Such a scenario can arise, for example, from a higher dimensional theory [12] after suitable choice of compactification.

III. MUON FLUX, SD CROSS SECTION AND CONVERSION FACTORS

In this section we will review the calculation of the muon flux and spin dependent cross section and revisit the way the conversion factors between the two are calculated. The IceCube collaboration [13] has presented its results as a future bound on the muon flux from the Sun. The bound was then converted to a bound on the spin dependent cross section by suitable conversion factors calculated in [14] and also discussed in [15].

The flux of neutrino induced muons from neutralino annihilation in the Sun is given by

$$\Phi_\mu = \frac{\Gamma_A \cdot n}{4\pi D_\odot^2} \int_{E_\mu^{th}}^\infty dE_\mu \int_{E_\mu}^\infty dE_\nu \int_0^\infty d\lambda \int_{E_\mu}^{E_\nu} dE'_\mu P_{\text{SURV}}(E_\mu, E'_\mu, \lambda) \times \frac{d\sigma_\nu(E_\nu, E'_\mu)}{dE'_\mu} \sum_i P_{\text{osc}}(\mu, i) \sum_f B_f \frac{dN_i^f}{dE_\nu}. \quad (5)$$

Here Γ_A is the annihilation rate, n is the target number density, and D_\odot is the distance from the center of the Sun to the detector. dN_i^f/dE_ν is the differential energy spectrum of the number of neutrinos from neutralino annihilation with the corresponding branching fractions B_f . E_μ^{th} is the threshold energy of the muon in the detector, λ is the muon range, $P_{\text{SURV}}(E_\mu, E'_\mu, \lambda)$ is the survival probability for a muon, $d\sigma_\nu(E_\nu, E'_\mu)/dE'_\mu$ is the differential neutrino cross-section and $P(\mu, i)$ is the oscillation probability for a neutrino of flavor i to oscillate to flavor μ in the detector.

The annihilation rate for the weakly interacting massive particles (WIMPs) in the center of the Sun is given by

$$\Gamma_A = \frac{1}{2} C_C \tanh^2(t/\tau), \quad (6)$$

$\tau = (C_C C_A)^{-1/2}$ is a measure of the time in which capture and annihilation equilibrate, C_C is the capture rate, and C_A parameterizes the annihilation rate of the WIMPs. For present WIMP annihilation rate, t is the age of the Sun, i.e., $t = t^\odot \simeq 4.5 \cdot 10^9$ years. The annihilation and capture rate are in equilibrium when $t^\odot/\tau \gg 1$, which implies

$$\Gamma_A = \frac{1}{2} C_C. \quad (7)$$

Since the capture rate is proportional to the spin dependent and spin independent cross sections, there would be a direct correlation between the flux and the SD cross section. The converted bound cannot be trusted for models where the equilibrium condition is not satisfied.

Accurate expressions for the capture rate can be found in [16], while reference [17] gives the approximate expressions. For the case of SD cross section, which occurs mainly on hydrogen and the form factor suppression is negligible, the capture rate in the Sun can be written as

$$C_{SD}^\odot = (1.3 \cdot 10^{23} \text{ s}^{-1}) \left(\frac{270 \text{ km s}^{-1}}{\bar{v}} \right) \left(\frac{\rho_\chi}{0.3 \text{ GeV cm}^{-3}} \right) \left(\frac{100 \text{ GeV}}{m_\chi} \right) \left(\frac{\sigma_{SD}}{10^{-40} \text{ cm}^2} \right) S(m_\chi/m_p), \quad (8)$$

where σ_{SD} is the neutralino-proton spin dependent cross section, $\bar{v} = 270 \text{ Km s}^{-1}$ is the dark matter velocity dispersion, $\rho_\chi = 0.3 \text{ GeV cm}^{-3}$ is the local dark matter density, and $S(m_\chi/m_p)$ is the kinematical suppression factor defined as

$$S(x) = \left(\frac{A^{3/2}}{1 + A^{3/2}} \right)^{2/3}, \quad (9)$$

with

$$A(x) = \frac{3x}{(x-1)^2} \left(\frac{\langle v_{esc}^2 \rangle}{\bar{v}^2} \right). \quad (10)$$

$\langle v_{esc} \rangle$ denotes the mean escape velocity from the Sun.

Reference [14] calculates accurate conversion factors including neutrino oscillations. Here we take a simple example to see how the conversion factors are calculated to get the SD cross section from the muon flux. Ignoring detector thresholds and taking the effective range of muons in the detector, the rate of neutrino induced through going muons for the Sun can be approximated as [17]

$$\Gamma_\mu \approx (1.27 \times 10^{-23} \text{ km}^{-2} \text{ yr}^{-1}) \frac{C_C}{s^{-1}} \left(\frac{m_\chi}{1 \text{ GeV}} \right)^2 \sum_i a_i b_i \sum_F B_f \langle N z^2 \rangle_{f,i}(m_\chi). \quad (11)$$

Since the capture in the Sun is mainly through spin dependent scattering, we can assume $\sigma_{SI} = 0$ ($C_C = C_{SD}^\odot$) to get a bound on the SD cross section. a_i are the neutrino scattering coefficients $a_\nu = 6.8$ and $a_{\bar{\nu}} = 3.1$, and b_i are the muon range coefficients with $b_\nu = 0.51$ and $b_{\bar{\nu}} = 0.67$. The quantity $\langle N z^2 \rangle_{f,i}$ is the second moment of the neutrino spectrum of type i from final state f , scaled by the square of the injection energy E_{in} of the annihilation products, and is given by

$$\langle N z^2 \rangle_{f,i}(m_\chi) = \frac{1}{E_{in}^2} \int \left(\frac{dN}{dE} \right)_{f,i} (E_\nu, E_{in}) E_\nu^2 dE_\nu. \quad (12)$$

The neutrino spectrum from the W^+W^- and $\tau^+\tau^-$ channels can be taken as [18]

$$\left(\frac{dN}{dE_\nu}\right)_{WW}^\odot = \frac{\Gamma_{W\rightarrow\mu\nu}}{E_{in}}(1 + E_\nu\tau_i)^{-\alpha_i-2}, \quad (13)$$

with $E_{in}(1 - \beta/2) \leq E_\nu \leq E_{in}(1 + \beta/2)$, $\Gamma_{W\rightarrow\mu\nu} = 0.105$, $\beta = (1 - m_W^2/E_{in}^2)^{1/2}$, $\tau_\nu = 1.01 \times 10^{-4}\text{GeV}^{-1}$ and $\tau_{\bar{\nu}} = 3.8 \times 10^{-4}\text{GeV}^{-1}$, and

$$\left(\frac{dN}{dE_\nu}\right)_{\tau^+\tau^-}^\odot = \frac{2\Gamma_{\tau\rightarrow\mu\nu\nu}}{E_{in}}(1 - 3x^2 + 2x^3)(1 + E_\nu\tau_i)^{-\alpha_i-2}, \quad (14)$$

with $0 \leq E_\nu \leq E_{in}$ $x = E_\nu/E_{in}$ and $\Gamma_{\tau\rightarrow\mu\nu\nu} = 0.18$, $\alpha_\nu = 5.1$ and $\alpha_{\bar{\nu}} = 9.0$. Note that improved functions for the spectra can be obtained by using programs like Pythia. In Fig. 1 we show plots of the second moment of these functions. We take $B_f = 1$ and only consider contributions of the hard channels W^+W^- and $\tau^+\tau^-$. In our plots we assume that only the W^+W^- channel contributes for $m_\chi > 80\text{ GeV}$, and the $\tau^+\tau^-$ channel for $m_\chi < 80\text{ GeV}$. The second moments $\langle Nz^2 \rangle_{WW}$ and $\langle Nz^2 \rangle_{\tau\tau}$ for the W^+W^- and $\tau^+\tau^-$ channels are obtained by inserting Eqs. (13) and (14) in (12). From Eq. (11),

$$\Gamma_\mu = (1.27 \times 10^{-23}\text{km}^{-2}\text{yr}^{-1}) \frac{C_{SD}^\odot}{s^{-1}} \left(\frac{m_\chi}{1\text{GeV}}\right)^2 [3.47\langle Nz^2 \rangle_{WW,\nu}(m_\chi) + 2.08\langle Nz^2 \rangle_{WW,\bar{\nu}}(m_\chi)], \quad (15)$$

for $m_\chi > (<)80\text{ GeV}$ for the W^+W^- ($\tau^+\tau^-$) channel.

We can re-write Eq. (8) as

$$C_{SD}^\odot = f_1(m_\chi)\sigma_{SD}, \quad (16)$$

and inserting this in Eq. (11) we have

$$\Gamma_\mu = f_1(m_\chi)f_2(m_\chi)\sigma_{SD}, \quad (17)$$

which yields the conversion factor

$$\frac{\sigma_{SD}}{\Gamma_\mu} = f_1^{-1}(m_\chi)f_2^{-1}(m_\chi)(\text{km}^2 \text{ yr cm}^2). \quad (18)$$

The conversion factor and the converted future IceCube/DeepCore bound obtained from it are plotted in Fig. 2. The conversion factor we find is similar to the estimates made in [14] without including neutrino oscillations. We will see later how the converted IceCube/DeepCore future bound for the SD cross section is changed once neutrino oscillations are included.

Neutrinos created from neutralino annihilations in the Sun's center may experience oscillations and interactions (neutral as well as charged) in the Sun. These and other factors, like the Solar composition, can modify the flux observed by detectors on Earth. On the other hand, direct detection involves measuring the scattering cross section of neutralinos off of nuclei. The conversion of the limit obtained from indirect detection experiments thus involves several uncertainties [14]. They include:

- Uncertainties in the Solar model.
- Gravitational effects of planets like Jupiter.
- Form factors.
- Variations in local dark matter density and velocity distributions.
- Neutrino oscillations.

These uncertainties can affect the estimated muon flux and thereby the deduced cross section. Gravitational affects from Jupiter, for example, can reduce the estimated muon flux, whereas neutrino oscillations can enhance it. The form factor suppression is negligible for the case of spin dependent interaction since the capture in the Sun mainly occurs through scattering on the hydrogen nuclei. All of the above listed affects can have implications for the particular particle physics model being investigated. The implications for our models are discussed in section V.

IV. PHENOMENOLOGICAL CONSTRAINTS AND SCANNING PROCEDURE

We use the package DarkSUSY-5.0.5 [19] to calculate the flux of neutrino induced muons from the Sun. DarkSusy (DS) uses a local dark matter density of $\rho_\chi = 0.3\text{ GeV}/\text{cm}^3$. From the three methods DS employs to calculate the relic density, we pick

the one which includes coannihilations only if the mass difference between the LSP and NLSP is less than 30%. We rescale the neutralino density to $\rho = \rho_0(\Omega h^2/0.025)$, for $\Omega h^2 < 0.025$. This is done because the neutralino cannot make up all of the dark matter in the galaxy halos if Ωh^2 drops below 0.025.

Although not required, we assume for simplicity, that the gauge coupling unification condition $g_1 = g_2 = g_3$ holds at M_{GUT} for FSU(5). DarkSUSY-5.0.5 uses Isajet 7.78 [20] for renormalization group evolution (RGE) running and the latter employs two loop MSSM RGEs and defines M_{GUT} to be the scale where $g_1 = g_2$. A few percent deviation from exact unification ($g_1 = g_2 = g_3$) can be attributed to unknown GUT-scale threshold corrections [21].

For the random scan we employ the following ranges for our parameters

$$\begin{aligned} 0 &\leq m_0 \leq 5 \text{ TeV}, \\ 0 &\leq M' \leq 1 \text{ TeV}, \\ 0 &\leq M_2 \leq 1 \text{ TeV}, \\ 0 &\leq m_A \leq 1 \text{ TeV}, \\ 0 &\leq \mu \leq 10 \text{ TeV}, \\ \tan\beta &= 10, 30, 50, \\ A_0 &= 0, \end{aligned} \tag{19}$$

we set $m_t = 173.1 \text{ GeV}$.

The random scan is performed over the parameter space of CMSSM ($M_2=M_3=M'=m_{1/2}$, $m_0=m_{H_u}=m_{H_d}$), FSU(5), NUHM2 ($M_2=M'$), and FSU(5) with universal soft Higgs masses² ($m_{H_u}^2=m_{H_d}^2$) at M_{GUT} . Since the neutralino mass is sensitive to the gaugino masses, we manipulate the latter to obtain more allowed points in the parameter space. We take piecewise intervals $[0,10]$, $[10,100]$ and $[100,1000]$ for the gaugino masses (in units of GeV). The random points in each of these intervals are distributed logarithmically. These points were then combined with a uniform distribution of points on the interval $[0,1000]$, with the total number of points around a million, which enables us to obtain a sufficiently dense set of points for our plots. This is still not sufficient for FSU(5)-UH, so we perform a Gaussian scan around the allowed points. The code makes a Gaussian distribution of points for the scalar and gaugino mass parameters around a point satisfying all the imposed constraints, with the variance and mean of the Gaussian distribution being 1/25 and 1 respectively. The random function RNORMX(), available in the program library of CERN, was used to make this Gaussian distribution.

We apply the experimental constraints on the data sequentially, with all of the collected data points satisfying the requirement of radiative electroweak symmetry breaking (REWSB), and the neutralino in each cases being the LSP. On this data, we impose the following constraints:

$$\begin{aligned} m_{\tilde{\chi}_1^\pm} \text{ (chargino mass)} &\geq 103.5 \text{ GeV} & [22] \\ m_{\tilde{\tau}} \text{ (stau mass)} &\geq 105 \text{ GeV} & [22] \\ m_{\tilde{g}} \text{ (gluino mass)} &\geq 250 \text{ GeV} & [22] \\ m_{\tilde{t}} \text{ (stop mass)} &\geq 175 \text{ GeV} & [22] \\ m_{\tilde{b}} \text{ (sbottom mass)} &\geq 222 \text{ GeV} & [22] \\ m_h \text{ (lightest Higgs mass)} &\geq 114.4 \text{ GeV} & [23] \\ BR(B_s \rightarrow \mu^+ \mu^-) &< 5.8 \times 10^{-8} & [24] \\ 2.85 \times 10^{-4} \leq BR(b \rightarrow s\gamma) &\leq 4.24 \times 10^{-4} \text{ (} 2\sigma \text{)} & [25] \\ \Omega_{\text{CDM}} h^2 &= 0.111^{+0.028}_{-0.037} \text{ (} 5\sigma \text{)} & [1] \end{aligned}$$

Note that we do not include the $(g-2)_\mu$ constraint for the rest of our discussion.

V. RESULTS

We next present the results from the scan over the parameter space listed in Eq. (19). In Fig. 3, we show how the converted IceCube/DeepCore future bound is altered with the inclusion of neutrino oscillations. The colored points are consistent with REWSB and satisfy the WMAP relic density bound in the 5σ range, particle mass bounds, and all constraints coming from the B-physics. We used different color coding to distinguish different channels for neutralino dark matter. We see from the right panel in Fig. 3, and as noted in reference [14], the inclusion of neutrino oscillations has a notable affect on the bound, especially for neutralino mass less than the W boson mass. As the W boson decouples ($m_\chi < 80 \text{ GeV}$) and the contribution from the tau channel becomes relevant, the bound changes notably. The reason for this is that the tau neutrinos from the decay $\tau^- \rightarrow \mu^- \bar{\nu}_\mu \nu_\tau$ can oscillate into muon neutrinos, thereby enhancing the muon flux in the detector. This is especially relevant for the low neutralino masses we have in FSU(5). In the left panel the future IceCube/DeepCore bound (solid line) indicates that the light neutralino ($m_\chi < 70 \text{ GeV}$) parameter space can be tested at IceCube/DeepCore detector, but this same region of the

parameter space, it seems, does not yield sufficient muon fluxes, as can be seen in the right panel of Fig. 3. So we see that there is some discrepancy.

Note that, whereas the calculation of the flux is sensitive to the various channels from which the neutrino arises, the cross section is not. Fig. 3 shows that as the neutralino mass falls below the W mass, and only soft channels (e.g. $b\bar{b}$) are left, the muon flux starts decreasing, whereas the SD cross section decreases much less rapidly [26]. This is because the SD cross section is not prone to the hardness or softness of the channel, which is not the case for the bound on the SD cross section where the sensitivity of the flux is translated to the SD cross section.

For the calculation of the flux we use the 'default' method in DS which uses the approximate expression for the capture rate in the Sun from [17]. It is understood that the dark matter prediction is no longer a natural consequence of supersymmetry [27], but requires special relations among the parameters. To have the correct relic dark matter abundance, we require coannihilation, resonance or specific Bino-Higgsino mixing solution. On the other hand this then yields some very specific structure for the sparticle spectroscopy which can be tested at the LHC. This explains why, in Figs. 4, 5 and 6, we show the various relic channels for neutralino dark matter. The colored points are consistent with REWSB and satisfy the WMAP relic density bound in the 5σ range, particle mass bounds, and all constraints from B-physics. Figs. 4, 5 and 6 present the muon flux induced by the neutrinos originating from annihilating neutralino dark matter in the center of the Sun, for $\tan\beta = 10, 30, 50$. The points shown satisfy the WMAP relic density bounds in the 5σ range. The calculated muon flux is integrated above a threshold energy of 1 GeV. From Figs. 4, 5 and 6, we observe that the IceCube/DeepCore detector can test the following neutralino dark matter scenarios: Bino-Higgsino dark matter, light Higgs resonance and finally the "non-identified channel", which is a combination of various channels. The points we designate as being non-identified means that the conditions we apply on the neutralino to be from all other channels are not satisfied. Thus an observed signal at the IceCube/DeepCore detector can narrow the probable neutralino dark matter candidates, and combining this with a signal from the LHC may help identify the nature of dark matter.

In Fig. 7 we show the results in the fundamental parameter planes. Here $M_{1/2}$ stands for the GUT scale universal gaugino mass in CMSSM and NUHM2, and M_1 is the Bino mass for FSU(5)-UH and FSU(5) plots, the expression for which is given in Eq. (3). The green points are consistent with REWSB and satisfy the WMAP relic density bound in the 5σ range, particle mass bound, and all constraints coming from B-physics. The red points are a subset of the green ones and give muon fluxes which can be tested at the IceCube/DeepCore experiment. The IceCube/DeepCore experiment, we see, can test a significant region of the flipped SU(5) parameter space.

In Figures 8, 9, 10 and 11 we show the results in m_A vs. m_χ , $m_{\tilde{\tau}}$ vs. m_χ , $m_{\tilde{t}}$ vs. m_χ and $m_{\chi_{1\pm}}$ vs. m_χ planes respectively. The color coding in these figures is the same as for Fig. 7. We can see that the FSU(5) model gives rise to signals, corresponding to a relatively light $\tilde{\tau}$ and m_A , which can be seen by the IceCube/DeepCore experiment. This is not the case for CMSSM and NUHM2 models.

For $\tan\beta = 10$ the lower mass bounds on the lightest neutralino for the four models (CMSSM, NUHM2, FSU(5)-UH and FSU(5)) are 76.7 GeV, 53.1 GeV, 32.2 GeV and 31.6 GeV respectively. This is consistent with a recent study [28] which found a lower bound of 28 GeV on the mass of the LSP neutralino. From Fig 5 we see that this neutralino in the CMSSM case comes from the focus point region and when the Bino or Higgsino mixing is large. For NUHM2, it is from the h-resonance channel, whereas for FSU(5)-UH it is from the "non-identified" region. We note that the muon flux is highest when the LSP dark matter neutralino is mainly Bino-Higgsino like, and this observation is valid for the CMSSM as well as for its extensions.

Note that the IceCube/DeepCore bound is a conservative one and the muon flux limits can be improved by an order magnitude [29]. As noted in [29] their are prospects of detecting the CMSSM focus point (FP) region in the IceCube/DeepCore experiment. This can also be seen in Figures 4-6 for the CMSSM. Going from CMSSM to FSU(5) changes this, and in addition to more points in the FP region we also have some points from the non-identified and h-resonance regions. The non-universality of the Higgs mass parameters opens up the A-funnel region where resonant annihilation occurs through the CP odd Higgs boson A. The Bino-Wino coannihilation [30] channel arises from the gaugino non-universality in Eq. (3) and occurs for $2M_2 \sim M_1$ at M_{GUT} . As we can see from the muon flux plots, this region of the parameter space is not detectable with the current IceCube/DeepCore experiment.

Finally, in TABLE I we present three FSU(5) benchmark points for $\tan\beta = 10, 30, 50$ which yield observable muon fluxes. The first point belongs to the stau coannihilation region, the second point is associated with the Bino-Higgsino dark matter with light charginos, and the third corresponds to the h-resonance region.

VI. CONCLUSIONS

We have considered indirect neutralino dark matter detection in two sets of supersymmetric flipped SU(5) models. These two sets of models have non-universal soft gaugino masses at M_{GUT} that are related by the underlying $SU(5) \times U(1)_X$ gauge symmetry. The supersymmetry breaking soft Higgs masses², associated with H_u and H_d , are equal at M_{GUT} in one set of models (FSU(5)-UH) but not in the other (FSU(5)). We have provided estimates of the flux, from annihilating neutralinos in the Sun, of neutrino induced muons, and considered prospects of detecting this flux in the IceCube/DeepCore detector. Some uncertainties arise in converting the muon flux into spin dependent neutralino-nucleon cross sections that we have briefly

discussed. We offer comparisons with previously studied CMSSM and NUHM2 models, and also highlight some benchmark models in flipped SU(5) with varying neutralino compositions which can be tested by the IceCube/DeepCore experiment. Our results for NUHM2, FSU(5)-UH and FSU(5) show more points above the projected IceCube limit compared to the CMSSM, and hence a greater prospect of detection. This is to be expected because the models are less constrained than the CMSSM and possess additional free parameters.

ACKNOWLEDGMENTS

We thank Hasan Yüksel for his helpful advice, discussions and collaboration in the early stages of this work. We are also grateful to Joakim Edsjö, Gustav Wikström and Stephano Profumo for discussions related to Darksusy and our results. We also thank Rizwan Khalid and Shabbar Raza Rizvi for very useful comments and suggestions. This work is supported in part by the DOE Grant No. DE-FG02-91ER40626 (M.A., I.G., and Q.S.) and GNSF Grant No. 07.462.4-270 (I.G.).

-
- [1] E. Komatsu *et al.* [WMAP Collaboration], *Astrophys. J. Suppl.* **180**, 330 (2009).
 - [2] J. L. Feng, arXiv:1003.0904 [astro-ph.CO]; G. Jungman, M. Kamionkowski and K. Griest, *Phys. Rept.* **267**, 195 (1996).
 - [3] T. M. f. Collaboration, arXiv:1012.0881 [astro-ph.HE].
 - [4] I. Antoniadis, J. R. Ellis, J. S. Hagelin, and D. V. Nanopoulos, *Phys. Lett.* **B194**, 231 (1987).
 - [5] B. Kyae and Q. Shafi, *Phys. Lett. B* **635**, 247 (2006); M. U. Rehman, Q. Shafi and J. R. Wickman, arXiv:0912.4737.
 - [6] I. Gogoladze, R. Khalid, S. Raza and Q. Shafi, *Mod. Phys. Lett. A*, **25**, 3371 (2010);
 - [7] For recent discussions see L. Roszkowski, R. Ruiz de Austri and R. Trotta, *JHEP* **0707** (2007) 075; A. Belyaev, S. Dar, I. Gogoladze, A. Mustafayev and Q. Shafi, arXiv:0712.1049 [hep-ph]. D. Feldman, Z. Liu and P. Nath, *JHEP* **0804**, 054 (2008); J. R. Ellis, K. A. Olive and P. Sandick, *JHEP* **0808**, 013 (2008) F. Feroz, B. C. Allanach, M. Hobson, S. S. AbdusSalam, R. Trotta and A. M. Weber, *JHEP* **0810**, 064 (2008); G. Barenboim, P. Paradisi, O. Vives, E. Lunghi and W. Porod, *JHEP* **0804**, 079 (2008); J. L. Kneur and N. Sahoury, *Phys. Rev. D* **79**, 075010 (2009).
 - [8] See for instance J. R. Ellis, S. F. King and J. P. Roberts, *JHEP* **0804**, 099 (2008); H. Baer, A. Mustafayev, E. K. Park and X. Tata, *JHEP* **0805**, 058 (2008) and references therein.
 - [9] For a partial list of references see A. De Rujula, H. Georgi, and S. L. Glashow, *Phys. Rev. Lett.* **45**, 413 (1980); H. Georgi, S. L. Glashow, and M. Machacek, *Phys. Rev.* **D23**, 783 (1981); S. M. Barr, *Phys. Lett.* **B112**, 219 (1982); J. P. Derendinger, J. E. Kim, and D. V. Nanopoulos, *Phys. Lett.* **B139**, 170 (1984); I. Antoniadis, J. R. Ellis, J. S. Hagelin, and D. V. Nanopoulos, *Phys. Lett.* **B194**, 231 (1987); J. L. Lopez, D. V. Nanopoulos, G. T. Park, X. Wang and A. Zichichi, *Phys. Rev. D* **50**, 2164 (1994); J. R. Ellis, G. K. Leontaris, S. Lola and D. V. Nanopoulos, *Phys. Lett. B* **425**, 86 (1998); Q. Shafi and Z. Tavartkiladze, *Phys. Lett.* **B448**, 46 (1999); J. Jiang, T. Li, D. V. Nanopoulos and D. Xie, *Phys. Lett. B* **677**, 322 (2009).
 - [10] A. H. Chamseddine, R. L. Arnowitt and P. Nath, *Phys. Rev. Lett.* **49**, 970 (1982). R. Barbieri, S. Ferrara, and C. A. Savoy, *Phys. Lett. B* **119**, 343 (1982); L. J. Hall, J. D. Lykken, and S. Weinberg, *Phys. Rev. D* **27**, 2359 (1983); E. Cremmer, P. Fayet, and L. Girardello, *Phys. Lett. B* **122**, 41 (1983); N. Ohta, *Prog. Theor. Phys.* **70**, 542 (1983).
 - [11] S. M. Barr and A. Khan, *Phys. Rev. D* **74**, 085023 (2006).
 - [12] See for instance J. Jiang, T. Li, D. V. Nanopoulos and D. Xie, *Nucl. Phys. B* **830**, 195 (2010).
 - [13] R. Abbasi *et al.* [ICECUBE Collaboration], *Phys. Rev. Lett.* **102**, 201302 (2009).
 - [14] G. Wikstrom and J. Edsjo, *JCAP* **0904**, 009 (2009).
 - [15] G. Wikstrom, Ph.D. thesis.
 - [16] A. Gould, *Astrophys. J.* **321**, 571 (1987).
 - [17] G. Jungman, M. Kamionkowski and K. Griest, *Phys. Rept.* **267**, 195 (1996). ; L. Bergstrom, *Rept. Prog. Phys.* **63**, 793 (2000). ; G. Bertone, D. Hooper and J. Silk, *Phys. Rept.* **405**, 279 (2005).
 - [18] G. Jungman and M. Kamionkowski, *Phys. Rev. D* **51**, 328 (1995).
 - [19] P. Gondolo, J. Edsjo, P. Ullio, L. Bergstrom, M. Schelke and E. A. Baltz, *JCAP* **0407**, 008 (2004); P. Gondolo, J. Edsjo, P. Ullio, L. Bergström, M. Schelke, E.A. Baltz, T. Bringmann and G. Duda, <http://www.darksusy.org>.
 - [20] H. Baer, F. E. Paige, S. D. Protopopescu and X. Tata, arXiv:hep-ph/0001086.
 - [21] J. Hisano, H. Murayama, and T. Yanagida, *Nucl. Phys.* **B402** (1993) 46. Y. Yamada, *Z. Phys.* **C60** (1993) 83; J. L. Chkareuli and I. G. Gogoladze, *Phys. Rev. D* **58**, 055011 (1998).
 - [22] K. Nakamura [Particle Data Group], *J. Phys. G* **37**, 075021 (2010).
 - [23] S. Schael *et al.* *Eur. Phys. J. C* **47**, 547 (2006).
 - [24] T. Aaltonen *et al.* [CDF Collaboration], *Phys. Rev. Lett.* **100**, 101802 (2008).
 - [25] E. Barberio *et al.* [Heavy Flavor Averaging Group (HFAG) Collaboration], arXiv:0704.3575 [hep-ex].
 - [26] Email correspondence with Joakim Edsjo and G. Wikstrom.
 - [27] N. Arkani-Hamed, A. Delgado and G. F. Giudice, *Nucl. Phys. B* **741**, 108 (2006); H. Baer, A. Mustafayev, E. K. Park and X. Tata, *JCAP* **0701**, 017 (2007).
 - [28] I. Gogoladze, R. Khalid, S. Raza and Q. Shafi, arXiv:1008.2765 [hep-ph]; D. A. Vasquez, G. Belanger, C. Boehm, A. Pukhov and J. Silk, arXiv:1009.4380 [hep-ph].

- [29] J. Ellis, K. A. Olive, C. Savage and V. C. Spanos, Phys. Rev. D **81**, 085004 (2010).
- [30] H. Baer, T. Krupovnickas, A. Mustafayev, E. K. Park, S. Profumo and X. Tata, JHEP **0512**, 011 (2005); H. Baer, A. Mustafayev, E. K. Park and S. Profumo, JHEP **0507**, 046 (2005). I. Gogoladze, R. Khalid and Q. Shafi, Phys. Rev. D **79**, 115004 (2009); Phys. Rev. D **80**, 095016 (2009).

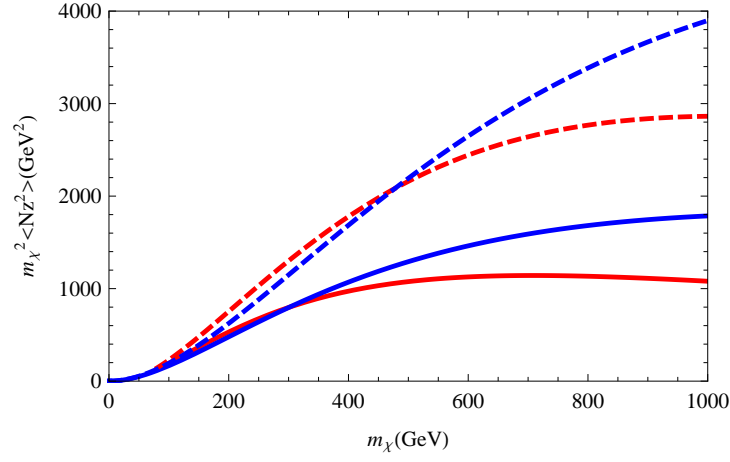


FIG. 1. Second moment of the neutrino spectrum. The solid lines correspond to neutrinos and the dashed lines are for anti-neutrinos. The W^+W^- channel is in red and $\tau^+\tau^-$ channel is in blue.

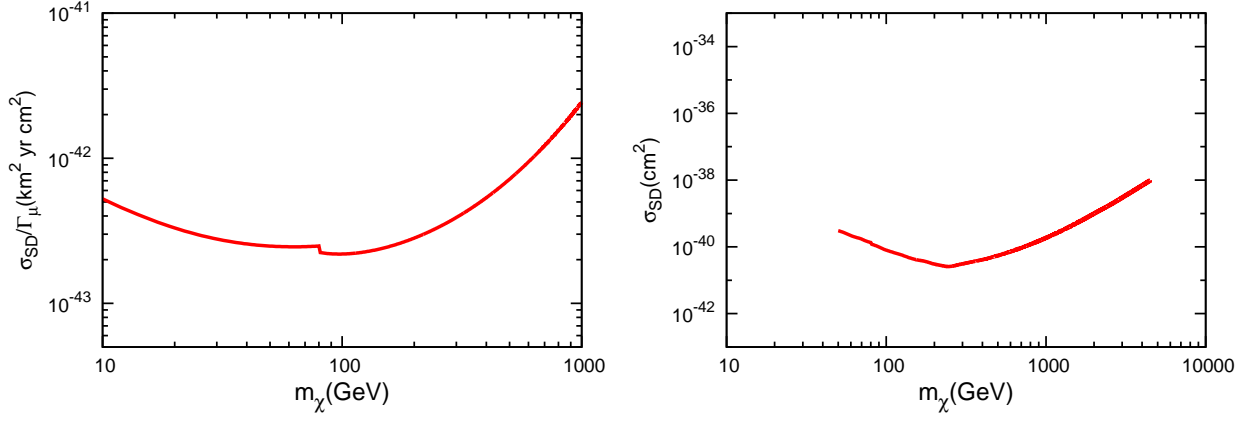


FIG. 2. The left panel shows the conversion factor calculated from approximate expressions for the flux and spin dependent cross section. The right panel shows the converted future IceCube/DeepCore muon flux bound using this conversion factor.

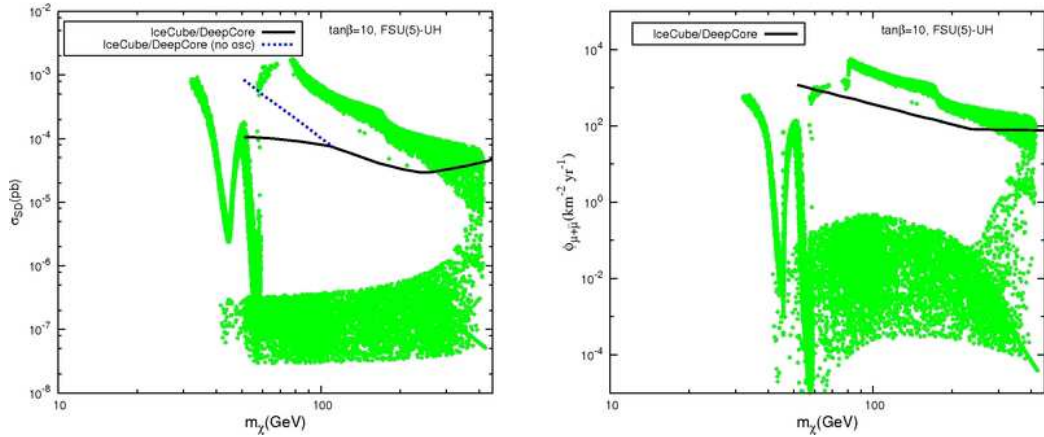


FIG. 3. Comparison of the future IceCube/DeepCore muon flux bound and the converted SD cross section bound. The muon flux is from the Sun above 1 GeV threshold is shown for $\tan\beta = 10$. The dashed line in the left panel is the future IceCube/DeepCore bound obtained if neutrino oscillations are not included in the flux calculation. The conversion factors used are given in reference [14].

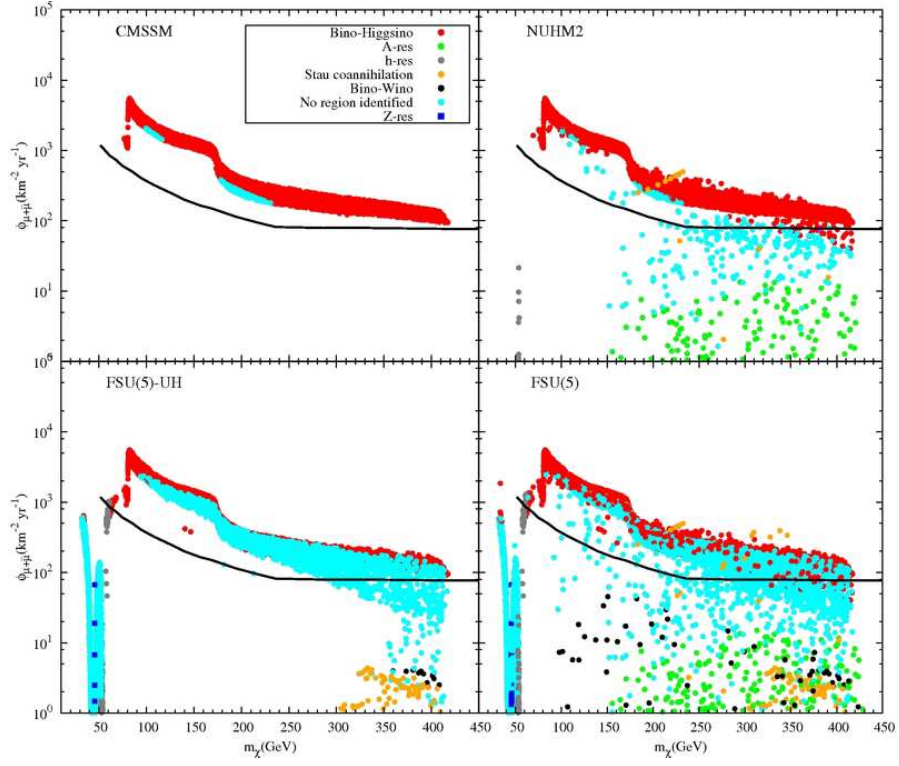


FIG. 4. Flux of $\mu + \bar{\mu}$ from the Sun above 1 GeV threshold for $\tan\beta = 10$. The black line shows the future IceCube/DeepCore bound [13]. The colored points are consistent with REWSB and satisfy the WMAP relic density bound in the 5σ range, particle mass bound, and all constraints coming from B-physics. The points in different colors correspond to the various solutions of LSP neutralino to be a dark matter candidate.

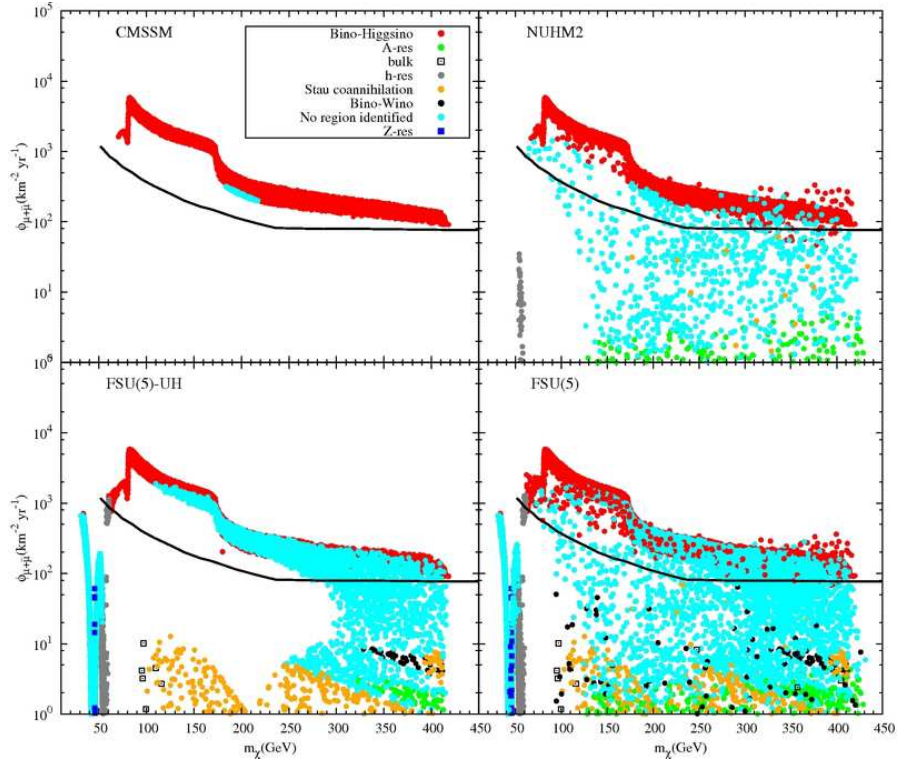


FIG. 5. Flux of $\mu + \bar{\mu}$ from the Sun above 1 GeV threshold for $\tan\beta = 30$. We use the same color coding as in Fig. 4.

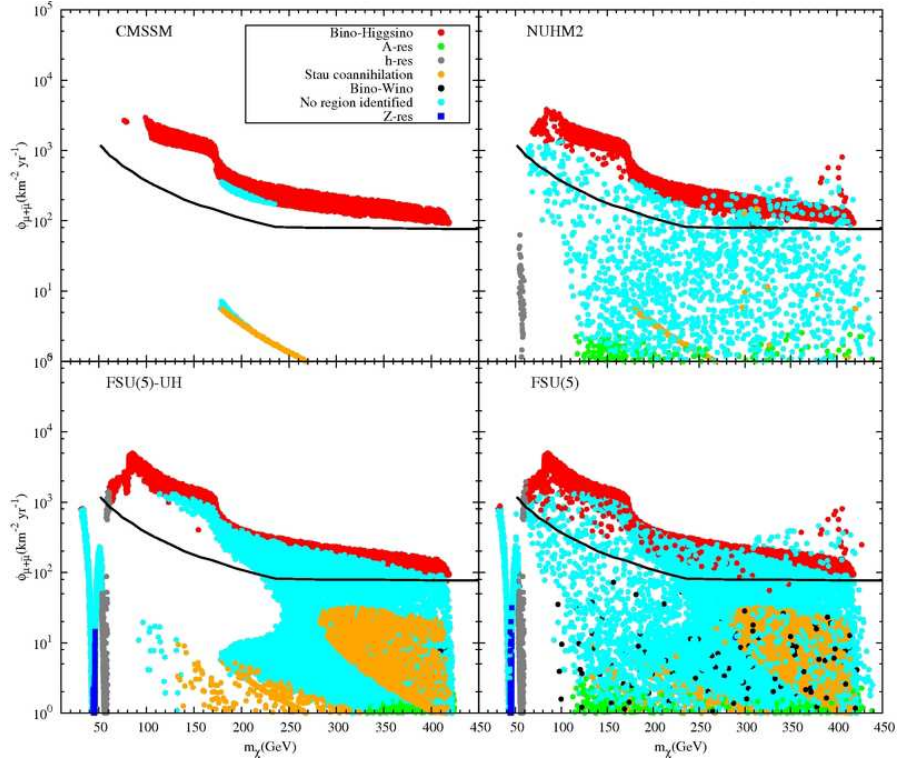


FIG. 6. Flux of $\mu + \bar{\mu}$ from the Sun above 1 GeV threshold for $\tan\beta = 50$. We use the same color coding as in Fig. 4.

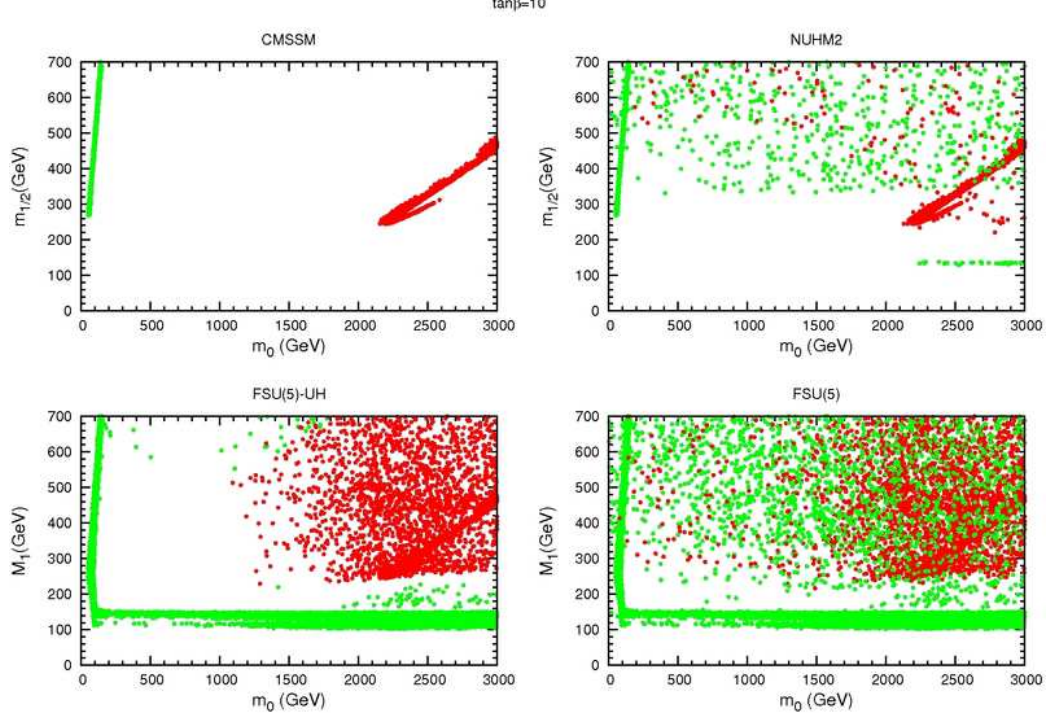
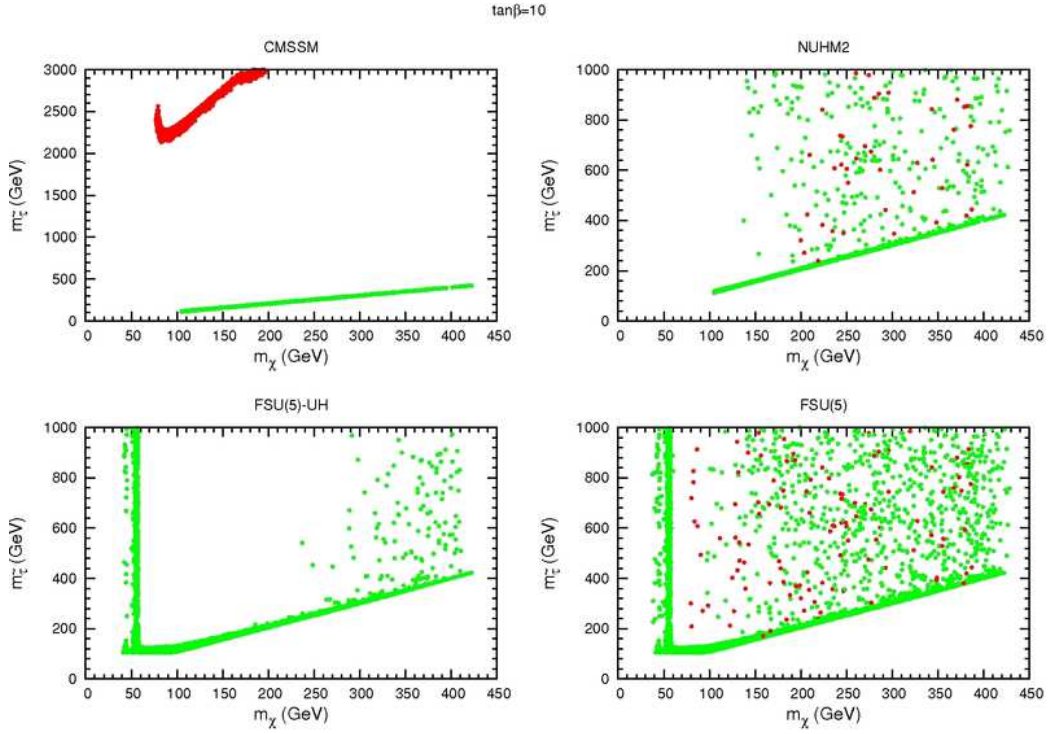
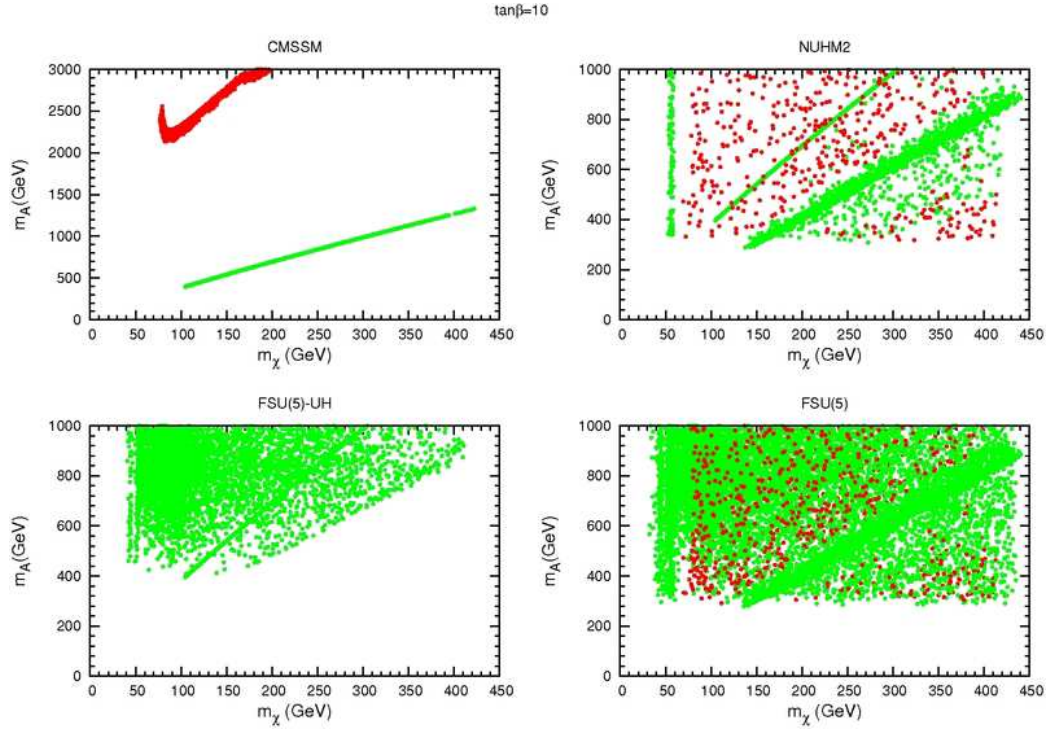


FIG. 7. Plot in the $m_{1/2}$ and M_1 vs m_0 plane. We are comparing the allowed parameter spaces for differed models. The green points are consistent with REWSB and satisfy the WMAP relic density bound in the 5σ range, particle mass bound, and all constraints coming from B-physics. The red points are a subset of the green ones and can generate detectable muon fluxes at the IceCube/DeepCore detector.



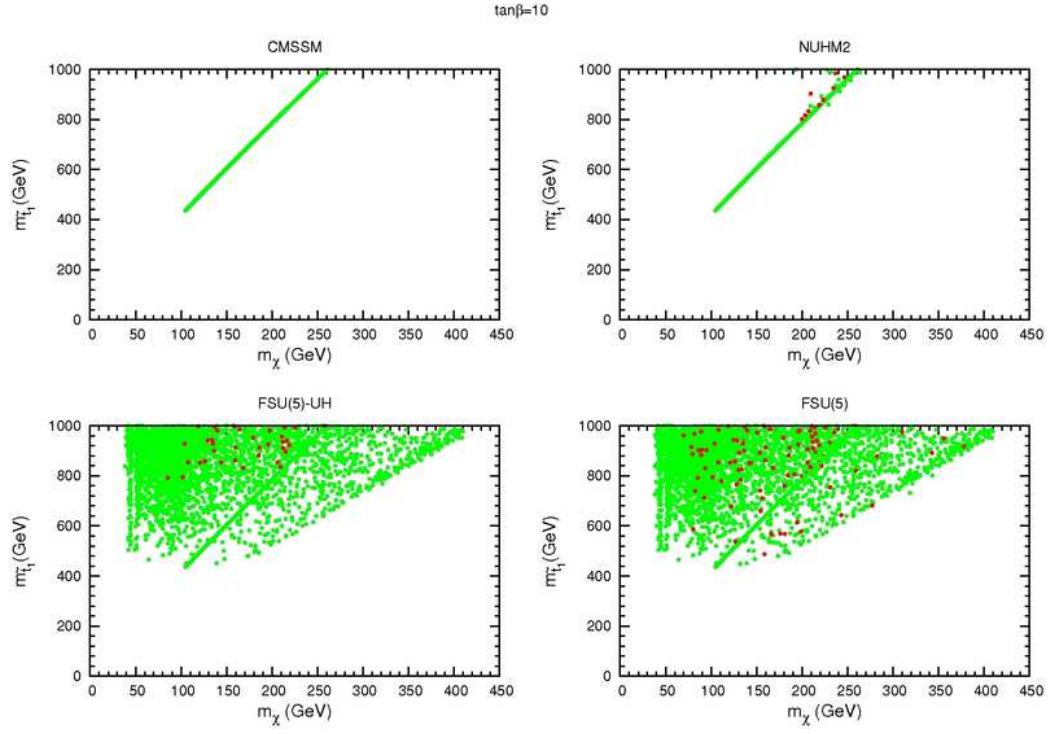


FIG. 10. Plot in the $m_{\tilde{t}_1} - m_\chi$ plane. Color coding same as in Fig. 7

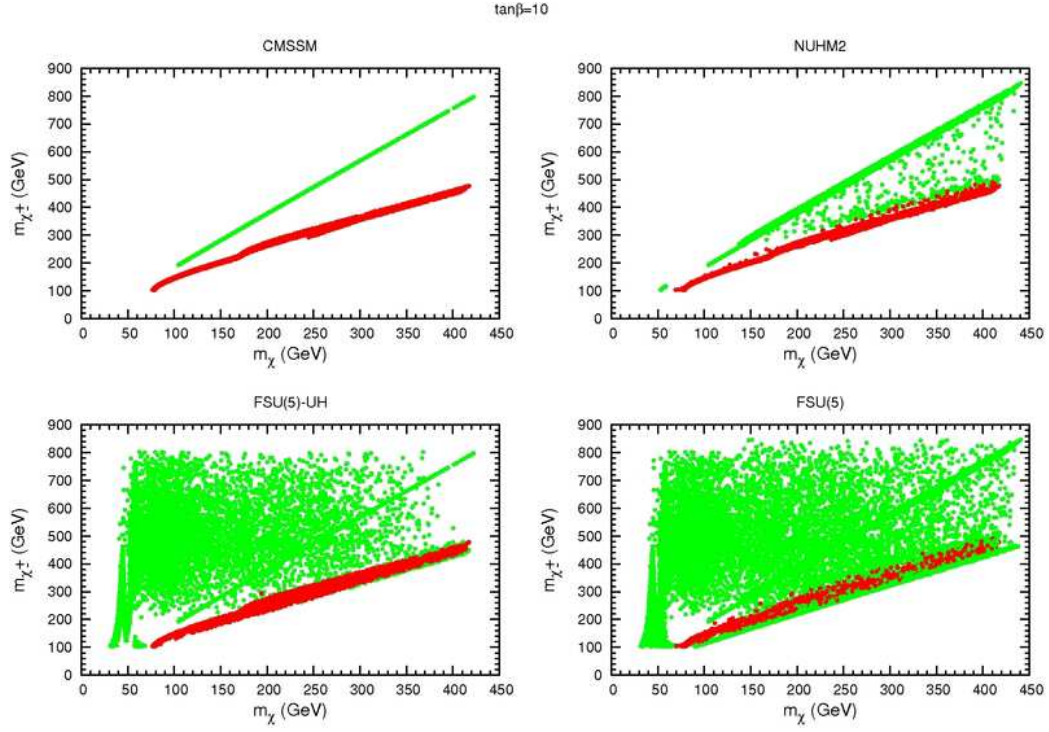


FIG. 11. Plot in the $m_{\chi^\pm_1} - m_\chi$ plane. Color coding same as in Fig. 7

	Point 1	Point 2	Point 3
m_0	107	1349	1335
M_1	691	295	176
M_2	607	848	519
M'	695	272	161
$\tan\beta$	10	30	50
A_0	0	0	0
μ	372	115	120
m_A	965	616	731
m_h	115	118	115
m_H	971	620	736
m_A	965	616	731
m_{H^\pm}	974	626	742
$m_{\tilde{\chi}_{1,2}^0}$	275,361	86,125	58,128
$m_{\tilde{\chi}_{3,4}^0}$	380,514	148,696	132,439
$m_{\tilde{\chi}_{1,2}^\pm}$	356,509	120,686	432,120
$m_{\tilde{g}}$	1369	1943	1263
$m_{\tilde{u}_{L,R}}$	1264,1220	2178,2146	1709,1683
$m_{\tilde{t}_{1,2}}$	900,1172	1493,1872	1124,1325
$m_{\tilde{d}_{L,R}}$	1267,1214	2179,2118	1711,1687
$m_{\tilde{b}_{1,2}}$	1140,1205	1852,2014	1301,1368
$m_{\tilde{\nu}_1}$	417	1473	1370
$m_{\tilde{\nu}_3}$	410	1433	1195
$m_{\tilde{e}_{L,R}}$	428,284	1476,1305	1373,1338
$m_{\tilde{\tau}_{1,2}}$	277,422	1211,1435	941,1196
$\sigma_{SI}(\text{pb})$	1.8×10^{-8}	7.65×10^{-8}	5.7×10^{-8}
$\sigma_{SD}(\text{pb})$	3.9×10^{-5}	9.75×10^{-4}	8.0×10^{-4}
$\Omega_{CDM}h^2$	0.075	0.077	0.093
$\phi_{\mu+\bar{\mu}}(\text{km}^{-2}\text{yr}^{-1})$	118	3728	1170

TABLE I. Sparticle and Higgs masses (in GeV), with $m_t = 173.1$ GeV. These benchmark points satisfy all the constraints imposed in Section V.